Comparison of several strategies for HEV energy management system including engine and catalyst temperatures

D. Maamria [1], F. Chaplais [2], N. Petit [2], A. Sciarretta [3]

Abstract— In this paper, we investigate the benefits of considering advanced modeling of engine and after-treatment system (3-way catalyst) in the design of Energy Management System (EMS) for a parallel Hybrid-Electric light-duty Vehicle (HEV) (passenger car with gasoline engine). The evaluation is based on a comparative study of optimal control problems formulated using three distinct levels of model complexity. Starting with a single state dynamics (battery state-of-charge), successively, we consider the engine temperature and the 3-way catalyst temperature, yielding increased complexity. As is shown, the increased complexity brings only little improvement in fuel economy and emissions reduction. We provide quantitative results to assess this observation.

I. INTRODUCTION

As is largely acknowledged, the Hybrid Electric Vehicle (HEV) technology is a major solution to reduce fuel consumption and pollutant emissions of passenger cars. Having two on-board energy sources provides a valuable degree of flexibility in the power generation. To handle this degree of freedom and coordinate the components of the power-train in an efficient manner, Energy Management Systems (EMSs) are used [6].

Common EMS are mostly based on heuristic considerations inspired by a priori knowledge of the behavior and the efficiency of the propulsion system [3], [4], [5], [12]. Lately, in an attempt to reach maximal levels of performance, optimization-based EMS have been introduced and studied [12], [15], [18], [20]. These strategies define a cost function to be minimized by a dynamical system representing the vehicle. For similar time horizons and driving conditions, various objectives and vehicle modeling levels can be considered. They result into distinct Optimal Control Problems (OCPs). Once solved, each OCP gives an optimal control strategy, to which corresponds an optimal cost value. The intrinsic difficulty of solving OCP in real time with guaranteed convergence and levels of performance has so far discarded them as true candidates for becoming real time EMS. However, should the complexity be alleviated, they would represent an appealing solution. A possible way to tame down the difficulty is to simplify OCPs formulations. Considering that more complex OCPs are usually more difficult to solve numerically and computationally more intense, some trade-off between optimality and model complexity can

be sought. In practice, an easy to compute and acceptably suboptimal solution is much more desirable than an optimal one characterized by an almost intractable OCP. This question of choosing the right level of modeling has been considered earlier. Various approaches from the literature and their results are summarized in Table I (upper part). To understand our aim in this paper, we now detail them, and list the employed state variables. To allow fair comparisons, we have reproduced the algorithms exposed in the literature and implemented them for one single example (detailed in this article).

In the simplest approaches, the battery State Of Charge (SOC), denoted by ξ, is usually the only state variable under consideration. Fuel consumption is the cost function. A final constraint on the SOC is introduced to reflect charge-sustaining (final SOC equals initial SOC) or charge-depleting operations (final SOC is nearly zero) [11], [12], [21]. The results obtained with one such EMS are reported in line (a) of Table I. Its consumption and emissions level will serve as references to the study conducted here.

Recent works have aimed at extending such simple optimization problems to consider new cost functions (pollutant emission, battery aging or any combination thereof) and additional state variables (engine, battery and the 3 way-catalyst temperatures) [9], [13], [19], [22]. From engine modeling viewpoint, engine temperature θ_e is an important factor [7], influencing both fuel consumption and pollutant emissions. This is particularly true for HEVs as the engine is subject to stop-start phases, and its temperature θ_e is not constant. However, several studies [9], [22] and [23] have suggested that the engine temperature could be eliminated from the state space, as it has a negligible influence on the results observed with EMS minimizing fuel consumption (the benefit of including engine temperature in term of fuel consumption is less than 0.5% for the systems studied in [9] and [23]). A theoretical justification of these results, reported in line (b) of Table I, are given in [10] based on regular perturbations in optimal control problems.

In the same spirit, the 3 way-catalyst temperature θ_c is also a key factor influencing pollutant emissions, as the catalyst is activated only after a certain threshold temperature is reached, while its efficiency is relatively poor at low temperatures [8], [11], [13]. However, only few works have included θ_c in the calculation of an EMS aiming at minimizing a trade-off between fuel consumption and pollutant emissions. In [2], [11] and [21], Pontryagin Minimum Principle (PMP) based optimization techniques including 3 way-catalyst dynamics with emissions as objective was presented along with

[1]D. Maamria is with IFP Energies Nouvelles and is PhD candidate in mathematics and control at CAS, MINES ParisTech `djamaleddine.maamria@mines-paristech.fr`.

[2]F. Chaplais and N. Petit are with CAS, MINES-ParisTech, 60 bd St Michel, 75272 Paris cedex, France.

[3]A. Sciarretta is with IFP Energies Nouvelles, 1-4 Av de Bois Préau, 92852 Rueil Malmaison, France.

TABLE I
COMPARISON OF VARIOUS TECHNIQUES (FROM LITERATURE AND IN THIS CONTRIBUTION)
ξ: STATE OF CHARGE OF THE BATTERY, θ_e: ENGINE TEMPERATURE AND θ_c: CATALYST TEMPERATURE.
THE EXPRESSION *Not satisfied* MEANS THAT THE STRATEGY CAN NOT REDUCE CO EMISSION BELOW 1 g/km

	Strategy	State variables	Min consumption in L/100km: CO $\leq$ 1 g/km	References	Optimal/Heuristic	Name
(a)	SOC ref	ξ	4.82 (*Not satisfied*)	[11], [12], [21]	Optimal	
(b)	Engine temp	ξ, θ_e	4.80 (*Not satisfied*)	[9], [22], [23]	Optimal	
(c)	Catalyst temp	ξ, θ_c	5.02	[2], [13], [14]	Heuristic	(S_4)
(d)	Catalyst+ engine temp	ξ, θ_e, θ_c	5.12	[11]	Heuristic	(S_3)
(e)	Contribution	ξ, θ_e, θ_c	4.86		Optimal	(S)
		ξ, θ_c	4.91		Optimal	(S_1)
		ξ	4.95		Optimal	(S_2)

numerical comparisons. In [13] and [14], the integration of the catalyst temperature in a gasoline-HEV EMS has been discussed using numerical comparisons between three control strategies, and, based on these numerical comparisons, a simplified control model has been suggested. The results are summarized in line (c) of Table I.

Finally, studies in [15] and [19] have quantified the impact of the battery temperature θ_{bat} on the EMS aiming at minimizing a trade-off between fuel consumption and battery aging [20]. The comparison in [19] of single state (SOC only) vs. two states (SOC+ θ_{bat}) solutions has shown that the first solution is sufficient in most cases, except in the case of the battery aging minimization.

This paper follows the path described above and extends it to new cases: more general cost function and more general choices of state variables. We consider a parallel Hybrid Electric Vehicle (passenger car equipped with gasoline engine). This choice is not restrictive, as the presented methodology could be transposed to other cases of interest. Assuming the model of the vehicle and the driving conditions are known, we address the following question: determine the optimal EMS which minimizes a trade-off between fuel consumption and pollutant emissions with SOC, engine and 3-way catalyst temperatures states. From the viewpoint of model complexity, we wish to select the right level of modeling to optimize the accuracy/complexity balance. A main motivation of this comparative study is to find a simplified model suitable for later real time implementation of OCP resolution. To be relevant for application, this simplified model should yield a reduction of CO emission below 1 g/km (which corresponds to the European norm Euro 6) with an acceptable extra fuel consumption.

In this article, we numerically show that the one state model given by the last line of Table I is in fact an adequate choice for the considered system, as it can be tuned to reach this goal.

The paper is organized as follows. In Section II, a mathematical control-oriented model taking into account the influence of engine and catalyst temperatures on the fuel consumption and pollutant emissions and the corresponding optimization problem are presented. Two simplifications of the general optimal control problem are given in Section III. On this basis, a PMP solution and the employed numerical method are described in Section IV. Finally, the obtained numerical results are presented and discussed in Section V and some conclusions and perspectives are drawn in Section VI.

II. CONTROL-ORIENTED MODEL

The system under consideration is a parallel hybrid-electric vehicle (HEV) equipped with gasoline engine and 3-way catalyst system. The specification of this HEV are listed in Table II. We assume that the vehicle follows a prescribed (known in advance) driving cycle. In the simulation, the NEDC cycle (see [6] and [23]) will serve as reference. Note that similar analysis has been done for another driving cycles: FUDS and FHDS.

A. Cost function

The cost function (1) to be minimized is a weighted sum of fuel consumption and pollutant emissions rate (out of the 3-way catalyst), over a fixed time window corresponding to a driving cycle of duration T.

$$J(u) = \int_0^T [(1-\alpha)c(u,t,\theta_e) + \alpha m_{CO}(u,t,\theta_e,\theta_c)]dt \quad (1)$$

In (1), $0 \leq \alpha \leq 1$ is a weighting factor serving to adjust the relative importance of the two contributions $c(.)$ and $m_{CO}(.)$, u is the control variable (the engine torque), θ_e is the engine temperature, θ_c is the 3-way catalyst temperature. The time variable t accounts for the dependence of the fuel consumption and CO emissions on the engine speed, which is a set path defined by the driving cycle to be tracked.

In (1), $c(.)$ is the instantaneous fuel consumption, which writes

$$c(u,t,\theta_e) = c_h(u,t)e(\theta_e)$$

where the function $c_h(.)$ is the fuel consumption rate for a warm engine. It is given by a quasi-steady map as a function of the engine speed and torque, which is derived from experimental engine tests (see Figure 4). The correction factor $e(.)$ of fuel consumption is a decreasing function of θ_e and is always greater than or equal to one. It represents the increase of friction and, as a consequence, the increase of fuel injected per cycle under low engine temperature conditions (see Figure 1). This function can be any decreasing (not necessarily smooth) function with asymptotic value of 1. In our case, the simple form reported in Figure 1 is extracted from the engine control maps given by car makers.
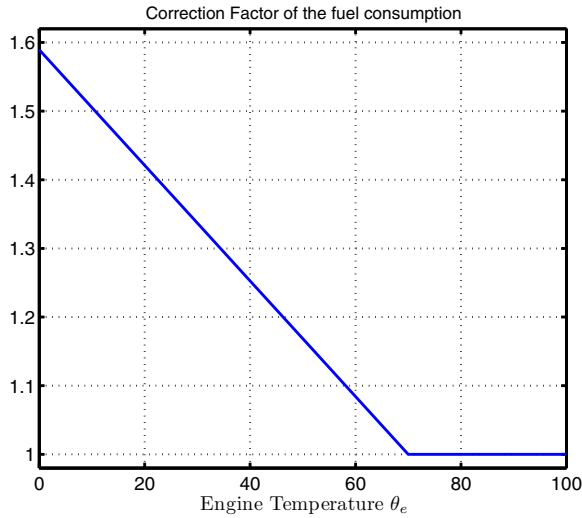
Fig. 1. The correction factor of fuel consumption $e(\theta_e)$

Similarly, the emission rate of CO out of the 3-way catalyst system $m_{CO}(.)$ is of the form

$$m_{CO}(u,t,\theta_e,\theta_c) = m_{CO,h}(u,t)e_{CO}(\theta_e)(1-\eta_{CO}(\theta_c))$$

where $m_{CO,h}$ is the emission rate out of the engine when the engine is warm, given by a quasi-steady map as a function of engine speed and torque. The correction factor $e_{CO}(.)$ of CO emissions is a decreasing function of θ_e and is always greater or equal to one. η_{CO} is the 3-way catalyst conversion efficiency for CO emissions (see Figure 2) which depends on the catalyst temperature θ_c.
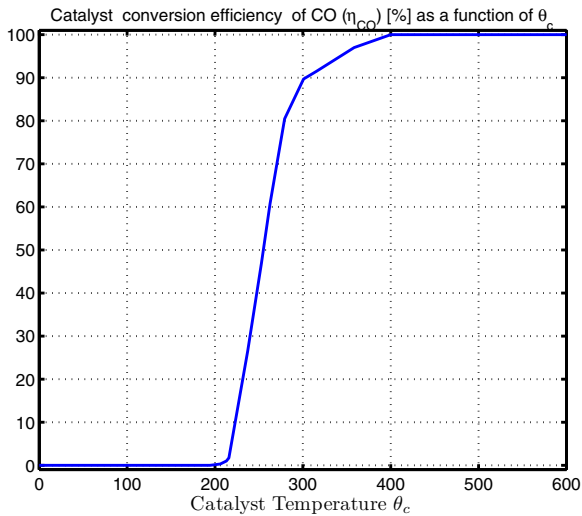

Fig. 2. 3-way catalyst conversion efficiency η_{CO} for CO emission

B. Dynamics

Three state variables are considered in the OCP formulations.

a) State Of Charge of the battery (ξ): The dynamics of the SOC, which describes the capacity remaining in the battery (expressed as a percentage of its nominal capacity) is given by

$$\dot{\xi} = -\frac{I_b(u,t,\xi)}{Q_0}, \quad \xi(0) = \xi_0$$

where I_b is the battery current intensity and Q_0 is the nominal battery capacity. The current is given by [6], [15]

$$I_b(u,t,\xi) = \frac{1}{2R_b(\xi)}\left(U_{oc}(\xi) - \sqrt{U_{oc}^2(\xi) - 4R_b(\xi)P_e(u,t)}\right)$$

where P_e is the electric power requested by the electric motor, R_b is the internal resistance of the equivalent circuit of the battery and U_{oc} is the equivalent open circuit voltage of the battery. The general expressions of R_b and U_{oc} are given in [6]. The value of P_e (which depends on the motor speed and torque) is determined from the total energy balance between the total power demand at the wheels P_d (which is assumed to be known as the driving cycle is known in advance) and the power provided by the engine P_{eng} (which depends on the engine speed and the engine torque) given by:

$$P_d = P_e + P_{eng}$$

One operational constraint for charge-sustaining HEVs requires that the final value of ξ should be equal to a target value, which is chosen here equal to the initial value

$$\xi(T) = \xi(0) \tag{2}$$

This final condition allows a fair comparison of the various solutions by guaranteeing that they reach the same level of battery energy at the end of the driving cycle. The current I_b depends on ξ, but we neglect this dependency as is commonly done in the literature [20]. In what follows, we shall write the dynamics of ξ and consider the initial condition ξ_0 as

$$\frac{d\xi}{dt} = f(u,t), \quad \xi(0) = \xi_0 \tag{3}$$

b) Engine Temperature (θ_e): The engine temperature satisfies the first order non-linear (balance) differential equation [11]

$$C_e\frac{d\theta_e}{dt} = P_{th,e}(u,t,\theta_e) - G_e \cdot (\theta_e - \theta_0) - P_{th,aux}$$

where C_e is an equivalent thermal capacity, G_e is an equivalent thermal conductivity, θ_0 is the ambient temperature, $P_{th,e}$ is the sum of friction power dissipated into heat and thermal power transferred from the engine to the coolant (given by a look-up table), and $P_{th,aux}$ is the thermal power drained by the cabin heater (it is considered constant). The model parameters have been identified using experimental data. In what follows, we shall write the dynamics of θ_e considering the initial condition θ_0 as the ambient temperature as

$$\frac{d\theta_e}{dt} = g(u,t,\theta_e), \quad \theta_e(0) = \theta_0 \tag{4}$$

c) 3-way catalyst temperature (θ_c): The third dynamics describes the evolution of the (spatially averaged) catalyst temperature θ_c. This lumped parameter is governed by a first order non-linear differential equation [21]

$$C_c(\theta_c) \cdot \frac{d\theta_c}{dt} = P_{th,ec} - P_{th,cr} - G_c \cdot (\theta_c - \theta_0) + P_{ch,c}$$

where C_c is an equivalent thermal capacity of the catalyst depending on θ_c, G_c in an equivalent thermal conductivity of the catalyst and θ_0 is the ambient temperature.

$P_{ch,c}$ is the heat released by chemical reactions in the after-treatment system. It depends on θ_e and θ_c [11]

$$P_{ch,c} = -\sum_j H_j \cdot \eta_j(\theta_c) \cdot m_{j,h}(u,t)e_j(\theta_e)$$

where $j = \{CO, HC, NOx\}$, and H_j is the heat generated by the oxidation of the jth pollutant.

$P_{th,ec}$ is the heat flux from the engine to the after-treatment system and $P_{th,cr}$ is the heat flux outside of the after-treatment system. These quantities are defined by

$$
\begin{aligned}
P_{th,ec} &= m_{exh} \cdot c_{exh}(\theta_{exh}) \cdot \theta_{exh} \\
P_{th,cr} &= m_{exh} \cdot c_c(\theta_c) \cdot \theta_c \\
m_{exh} &= c(u,t,\theta_e) \cdot \left(\frac{AFR_{st}}{\phi} + 1\right)
\end{aligned}
$$

where AFR_{st} is the stoichiometric value of the air/fuel ratio and ϕ is the equivalence ratio. c_{exh} and c_c are specific heat; they are functions of the exhaust temperature θ_{exh} (which is a (static) function of the engine speed and torque) and the catalyst temperature θ_c respectively. In what follows, we shall write the θ_c dynamics and consider the initial condition $\theta_c(0) = \theta_{c,0}$ under the form

$$\frac{d\theta_c}{dt} = k(u,t,\theta_e,\theta_c), \quad \theta_c(0) = \theta_{c,0} \tag{5}$$

An important remark is that the SOC dynamics (3) is independent from (θ_e, θ_c) and the θ_e dynamics is independent from (θ_c, ξ).

C. Constraints

Without loss of generality, the control u is constrained to belong to a functional space subset $U^{ad} \subset L^\infty[0,T]$ defined

$$u_{min}(t) \leq u(t) \leq u_{max}(t), \quad \text{for almost all} \quad t \in [0,T] \tag{6}$$

where the bounds are determined by the driving conditions, and physical limitations of the engine and the electric motor.

In summary, we can now formulate our OCP

$$(OCP) \quad \min_{u \in U^{ad}} J(u) \tag{7}$$

under the boundary constraint (2) and the dynamics (3, 4, 5). The corresponding optimal energy management strategy is denoted by (S).

III. SIMPLIFICATIONS OF THE (OCP)

In this section, two simplified control strategies of the strategy (S) described by the OCP (7), based on simplifying the factors $e(.)$, $e_{CO}(.)$ and $\eta_{CO}(.)$, are presented. Our aim is to find a reduced control model allowing us to get an acceptable sub-optimal solution. This model will be used as a benchmark to find a suitable real time strategy.

A. First simplification

The first simplification is to assume that the engine is warm and its temperature θ_e is always greater than $70°C$. This assumption is equivalent to neglecting the impact of θ_e in the case of engine cold start. This can be formulated

$$e_{CO} = 1, \ e = 1$$

The simplified cost is given by

$$J_1(u) = \int_0^T [(1-\alpha)c_h(u,t) + \alpha m_{CO,h}(u,t)(1-\eta_{CO}(\theta_c))]dt$$

As the cost is independent from θ_e, only the dynamics of SOC and θ_c (2 states) have to be considered with the final constraint (2). This simplified strategy is noted (S_1).

B. Second simplification

An additional possibility to simplify the strategy (S_1) is to assume that the catalyst is never activated and its efficiency η_{CO} is zero. The cost function, in this case, boils down to

$$J_2(u) = \int_0^T [(1-\alpha)c_h(u,t) + \alpha m_{CO,h}(u,t)] \, dt$$

On the other hand, assuming that the catalyst is activated and its efficiency is $\eta_{CO} = 1$ would give us a cost function depending only on fuel consumption and no reduction of pollutant emissions can be considered. That is why we have chosen (conservatively) to take $\eta_{CO} = 0$. This simplification is equivalent to minimize the CO emissions out of the engine.

As the fuel consumption and the pollutant emissions are independent from θ_c, the number of states can be reduced to 1. Only the dynamics of SOC, given by (3), has to be considered with the final constraint (2). We note this simplified strategy (S_2).

Note that these simplified strategies are only used to calculate the control trajectories as shown in Table IV. For the comparison between the different obtained strategies, we use the full model given by equations (1, 3, 4, 5).

IV. MATHEMATICAL AND NUMERICAL SOLVING

The OCP defined in (7) can be solved using numerous methods. Classically, the solution considered here is based on Pontryagin Minimum Principal (PMP) [1], [16]. We define the Hamiltonian H by

$$H = L(u,t,\theta_e,\theta_c) + \lambda f(u,t) + \mu g(u,t,\theta_e) + \rho k(u,t,\theta_e,\theta_c)$$

where λ, μ, ρ are the adjoint variables associated to ξ, θ_e and θ_c, respectively and L is given by

$$L(u,t,\theta_e,\theta_c) = (1-\alpha)c(u,t,\theta_e) + \alpha m_{CO}(u,t,\theta_e,\theta_c).$$

For a given control u^*, the adjoint states $\lambda(t)$, $\mu(t)$ and $\rho(t)$ are defined by

$$\frac{d\lambda}{dt} = -\frac{\partial H}{\partial \xi} = 0, \; \frac{d\mu}{dt} = -\frac{\partial H}{\partial \theta_e}, \; \frac{d\rho}{dt} = -\frac{\partial H}{\partial \theta_c} \quad (8)$$

with

$$\mu(T) = 0, \; \rho(T) = 0 \quad (9)$$

since the final temperatures $\theta_e(T)$ and $\theta_c(T)$ are free and the final time T is fixed. On the other hand, we have no boundary condition on λ since the final SOC is fixed.

From the PMP, if u^* is an optimal control, then, for every t, $u^*(t)$ minimizes the Hamiltonian in the set defined by (6) along the optimal states and corresponding adjoint states trajectories

$$u^* \in \arg\min_{u \in U^{ad}} H(u, t, \theta_e, \theta_c, \lambda, \mu, \rho) \quad (10)$$

Equations (3, 2, 8, 9, 10) constitute a two-point boundary value problem (TPBVP), denoted by (Σ). The same method can be used for the two strategies (S_1) and (S_2) and we note (Σ_1) and (Σ_2) their associated TPBVPs, respectively. To obtain conclusions on the relevance of the two levels of simplification above, we follow the procedure below:

- Compute the solution u^* for the optimal control problem (7) by solving the TPBVP (Σ).
- Compute optimal controls u_1^* and u_2^* for the simplified strategies (S_1) and (S_2) by solving the associated TPBVPs (Σ_1) and (Σ_2) respectively.
- Compare $J(u^*)$, $J(u_1^*)$ and $J(u_2^*)$. More than the obvious observation that $J(u^*) \leq J(u_1^*) \leq J(u_2^*)$, the question that we will study numerically is: how great is the difference between the three costs? The answer of this question will help us to decide the most convenient level of model complexity.

For the numerical solution of the TPBVPs, we have chosen to use a shooting method [1], [17]. Classically, the idea of this algorithm is to consider the initial conditions of the adjoint states $(\lambda_0, \mu_0, \rho_0)$ as unknown variables and the vector function which associates $[\xi(T) - \xi(0)]$, $\mu(T)$ and $\rho(T)$ to $(\lambda_0, \mu_0, \rho_0)$. Then, the problem is recast into finding zeros of this function from R^3 into R^3. This is achieved here using a Newton method implemented in the `fsolve` Matlab function.

V. NUMERICAL RESULTS

Simulation results are obtained for a parallel hybrid electric vehicle equipped with gasoline engine and 3-way catalyst system whose characteristics are listed in Table II. Look-up tables for fuel consumption $c_h(.)$, CO emissions $m_{CO,h}(.)$ and electric power $P_e(.)$ of the motor, illustrated in Figures 3, 4 and 5 respectively, are derived from experimental tests. The engine parameters are listed in Table III. According to Figure 1, the correction factor $e(.)$ and $e_{CO}(.)$ are of the form

$$\begin{cases} -a\theta_e + b, & \text{if } \theta_c \leq \theta_e \leq \theta_w \\ 1, & \text{if } \theta_e > \theta_w \end{cases}$$

TABLE II

VEHICLE CHARACTERISTICS

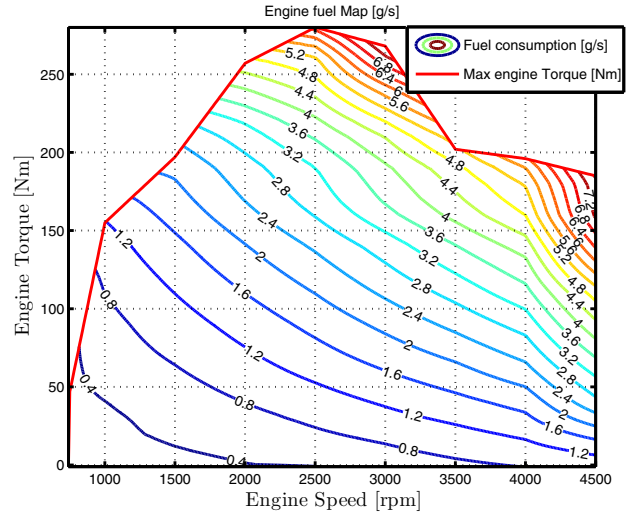| Vehicle weight	1932 kg
Engine max. power	92 kW
Motor max. power	42 kW
Battery capacity	5 Ah

Fig. 3.   Engine Fuel map $c_h(.)$ [g/s]

where a and b are positive constants. We note (a_0, b_0) and (a_1, b_1) coefficients associated to $e(\theta_e)$ and $e_{CO}(\theta_e)$ respectively.
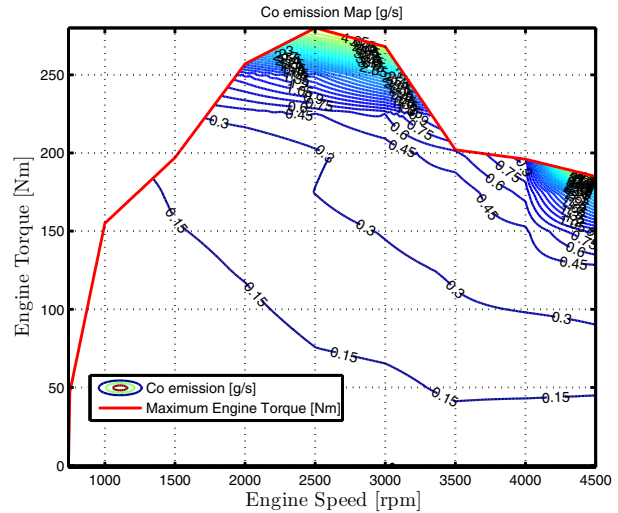

Fig. 4.   CO map $m_{CO,h}(.)$ [g/s]

For completeness of comparison, two additional heuristic strategies based on optimization are considered.

- The first one, noted by (S_3), is a pseudo solution of the TPBVP (Σ) where we impose $\mu(t) \equiv \rho(t) \equiv 0$ in the Hamiltonian H (see [11]). The only unknown variable λ is determined to satisfy the final constraint on ξ.
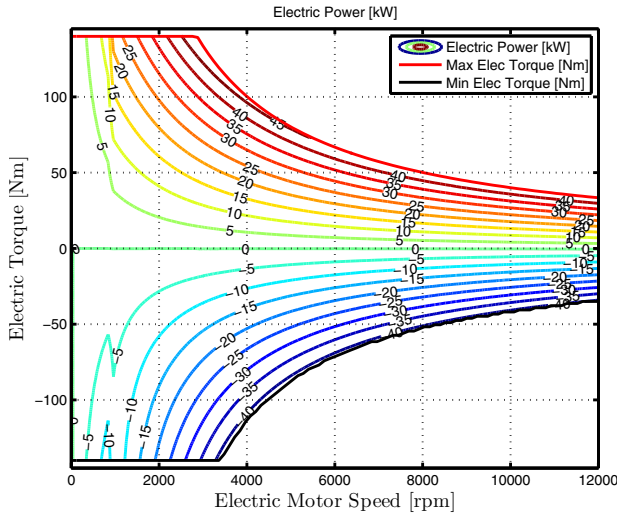- The second strategy, noted by (S_4), is the simplified strategy suggested in [13] and [14]: one neglects the

Fig. 5. Electric motor power $P_e(.)$ map [kW]

TABLE III

ENGINE PARAMETERS

Parameter	Value
a_0	$0.0084 \ [^\circ C]^{-1}$
b_0	1.59
a_1	$0.012 \ [^\circ C]^{-1}$
b_1	1.88
C_e	10^5 J/kg
G_e	$14.3 \ s^{-1}$
θ_w	$70 \ ^\circ C$
θ_c	$-30 \ ^\circ C$

impact of the engine temperature on fuel consumption and CO emissions (which is equivalent to assuming that the engine is warm) and we set $\rho(t) \equiv 0$ in the Hamiltonian. The only unknown variable λ is determined to satisfy the final constraint on ξ.

The calculation of the control trajectories for each strategy defined above are summarized in Table IV.

The simulated engine and the catalyst temperatures trajectories for $\alpha = 0.8$ by using all the strategies described before are reported in Figures 6 and 7 respectively. In Figure 6, one can note that the engine temperature trajectories for the three strategies $(S, \ S_1, \ S_2)$ remain close while the engine temperature trajectories are a little bit far from the optimal trajectory when the strategies $(S_3, \ S_4)$ are employed. From Figure 7, one can see that the optimal control u^* improves the catalyst efficiency by warming it up promptly, which decreases the pollutant emissions out of the catalyst. The price to pay for achieving this is an increased fuel consumption due to an increased use of the engine.

Figure 8 reports the values of the cost function J obtained by solving the previous optimal control problems for NEDC driving cycle for various values of $\alpha \in [0, \ 0.8]$. Note that we have obtained similar results for 3 other driving cycles: FUDS, FHDS, FTP. The two costs $J(u_1^*)$ and $J(u_2^*)$ are close to the optimal value $J(u^*)$ for the considered values of α: the relative error between $J(u^*)$ and $J(u_1^*)$ is less than
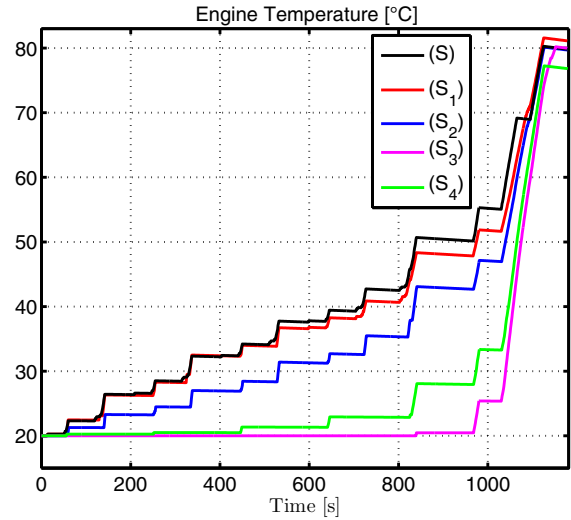

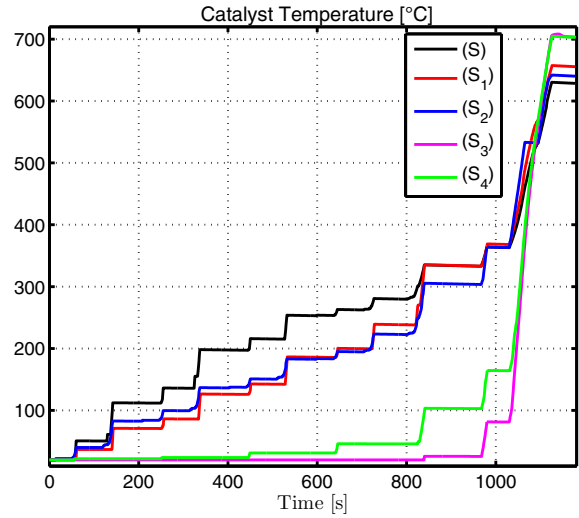Fig. 6. Histories of simulated engine temperature θ_e for $\alpha = 0.8$.

Fig. 7. Histories of simulated catalyst temperature θ_c for $\alpha = 0.8$.

2% and the relative error between $J(u^*)$ and $J(u_2^*)$ is less than 4% for the whole range $\alpha \in [0, \ 0.8]$. The difference between the three values of the cost increases when α tends to 1 (as more emphasis is put on on the minimization of CO emissions).

Figure 9 details the variation of the fuel consumption as a function of CO emissions for various values of α. One can see that the five strategies allow to reduce the CO emission below 1 g/km (which corresponds to the new European norm Euro 6 for CO emissions) while the main difference between them is in the fuel consumption value. The solutions corresponding to the strategies (S), (S_1) and (S_3) are very close in term of CO emissions reduction while the strategies $(S_2, \ S_4)$ are less efficient. If one desires to reduce CO emissions further using strategies $(S_2, \ S_4)$, one has to increase the value of α (recall that, in general, when the value of α in increased, more importance to CO emission is given in the cost function).

TABLE IV

CONTROL STRATEGIES DESCRIPTIONS

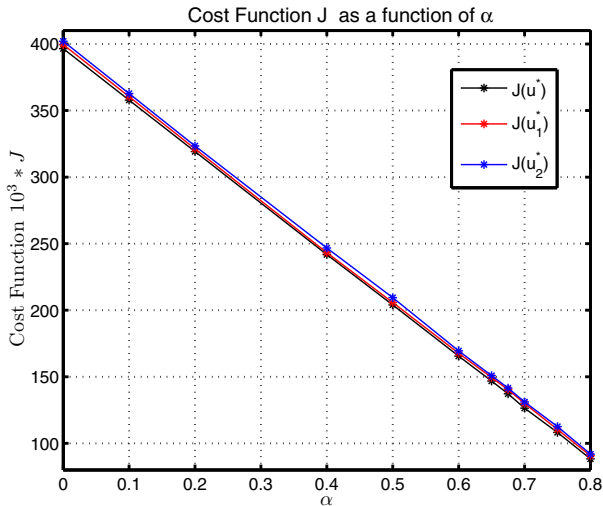| Strategy	Number of state variables	Control calculation	Optimal/Heuristic
(S)	3 (ξ, θ_e, θ_c)	$u^*(t) = \arg \min_{u \in U^{ad}} \underbrace{[L(u,t,\theta_e,\theta_c) + \lambda f(.) + \mu g(.) + \rho k(.)]}_{H(u,t,\theta_e,\theta_c,\lambda,\mu,\rho)}$	Optimal
(S_1)	2 (ξ, θ_c)	$u_1^*(t) = \arg \min_{u \in U^{ad}} \underbrace{[L(u,t,\theta_e = \theta_w,\theta_c) + \lambda f(.) + \rho k(.)]}_{H(u,t,\theta_e=\theta_w,\theta_c,\lambda,\mu(t)=0,\rho)}$	Optimal
(S_2)	1 (ξ)	$u_2^*(t) = \arg \min_{u \in U^{ad}} \underbrace{L(u,t,\theta_e = \theta_w,\theta_c = \theta_c(0)) + \lambda f(.)}_{H(u,t,\theta_e=\theta_w,\theta_c=\theta_c(0),\lambda,\mu(t)=0,\rho(t)=0)}$	Optimal
(S_3)	1 (ξ)	$u_3^*(t) = \arg \min_{u \in U^{ad}} \underbrace{[L(u,t,\theta_e,\theta_c) + \lambda f(.)]}_{H(u,t,\theta_e,\theta_c,\lambda,\mu(t)\equiv 0,\rho(t)\equiv 0)}$	Heuristic
(S_4)	1 (ξ)	$u_4^*(t) = \arg \min_{u \in U^{ad}} \underbrace{[L(u,t,\theta_e = \theta_w,\theta_c) + \lambda f(.)]}_{H(u,t,\theta_e=\theta_w,\theta_c,\lambda,\mu(t)=0,\rho(t)\equiv 0)}$	Heuristic

Fig. 8.   Cost function J as a function of α.

A main objective is to find a simple model allowing to reduce CO emissions below 1 g/km with an acceptable extra fuel consumption in exchange of ease of numerical complexity. This simplified model could be used for real time EMS calculation. From Figure 9, one can see that one state models corresponding to the strategies $(S_2,\ S_3,\ S_4)$ satisfy these requirements for $\alpha \geq 0.8$ while the difference between the values of consumed fuel is negligible only for S_2.

- The strategy (S_3) is far from the optimal fuel consumption (the difference is more than 5%).
- The strategy (S_4) is close to the optimal fuel consumption (the sub- optimality is less than 2%).
- The strategy (S_2) is better than the strategy (S_4) suggested in [13] and [14] as it gives a quasi-optimal fuel consumption comparing to the optimal strategy.

Therefore, we deduce that one can use the one state OCP strategy (S_2) to generate a control which satisfies the European norm Euro 6 for the CO emissions with a near to optimal fuel consumption. This simplified model used in this strategy will serve as a benchmark to find a suitable real time energy management system. We can for example use

the ECMS as it is presented in the literature to solve this one state problem.

The main idea of this article is to show how one can use optimal control as a numerical tool to determine a trade-off between model complexity and the optimality of the solution for hybrid electric vehicles. The presented method is not restrictive for the chosen system (parallel HEV with gasoline engine and 3 way catalyst), as the methodology could be transposed and adapted to more complicated cases.

VI. CONCLUSION

Usually, optimal control methods, when used on nonlinear dynamics are considered as relatively complex methods, which, in turn, as often discarded them from real time implementation. This is particularly true when on-board processing power is limited, as well as memory space that could be used to store pre-calculated initial solutions covering a wide-range of needs and operating conditions. However, when used off-line, they provide a fair methodology of comparisons between modeling approaches and allow to determine a trade-off between model complexity and optimality. This is what has been done in this contribution, and the result is that, for a HEV of parallel type equipped with gasoline engine and 3 way catalyst, one can conclude that the simplest model among all possible choices is accurate enough to guarantee a good level of emission reduction (meeting Euro 6 requirements) while reaching a quasi-optimal fuel efficiency. The Equivalent Consumption Minimization Strategy (ECMS) can be used to solve this kind of problem in real time. An experimental validation of the proposed solution is planned and is the subject of current investigation.

REFERENCES

[1] A. E. Bryson and Y. C. Ho. *Applied optimal control*. Ginn and Company: Waltham, MA, 1969.
[2] A. Chasse, G. Corde, A. Del Mastro, and F. Perez. Online optimal control of a parallel hybrid with after-treatment constraints integration. *IEEE Vehicle Power and Propulsion Conference*, pages 1–6, 2010.
[3] J. S. Chen and M. Salman. Learning energy management strategy for hybrid electric vehicles. *IEEE Conference Vehicle Power and Propulsion*, pages 68 – 73, 2005.
[4] S. Delprat, T. M. Guerra, and J. Rimaux. Control strategies for hybrid vehicles: Synthesis and evaluation. *In Proceedings of the Vehicular Technology Conference*, 5:3246–3250, 2003.
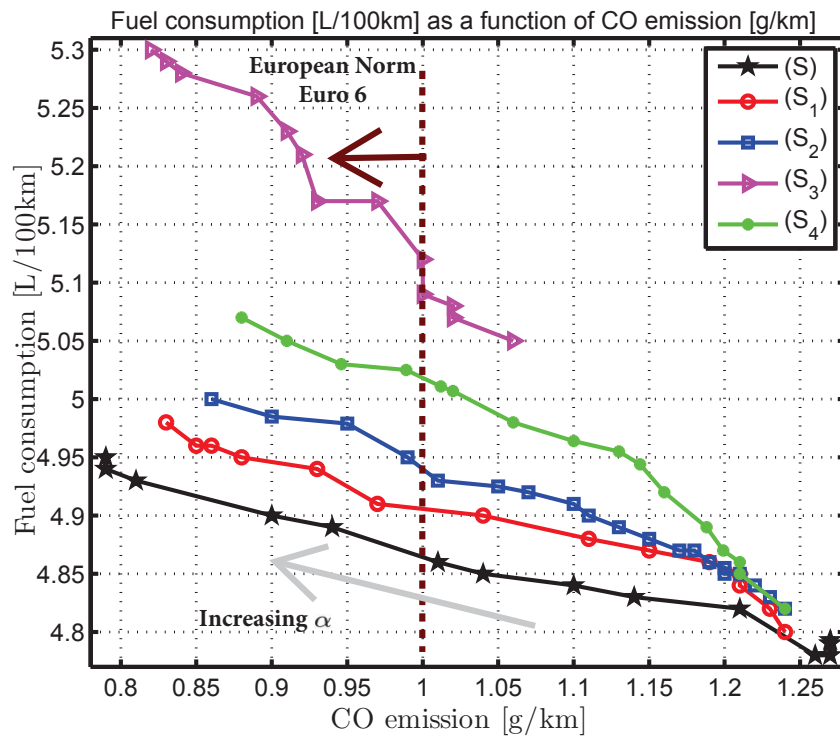
Fig. 9. Fuel consumption [L/100km] as a function of CO emissions [g/km]. For each policy, each point is obtained as follows: we fix the value of α and solve the problem corresponding to the strategies (S, S_1, S_2, S_3, S_4). The corresponding fuel consumption and CO emissions are presented.

[5] Y. Gaoua, S. Caux, P. Lopez, and J. D. Salvany. On-line HEV energy management using a fuzzy logic. *International Conference on Environment and Electrical Engineering*, pages 46 – 51, 2013.

[6] L. Guzzella and A. Sciarretta. *Vehicle Propulsion Systems: Introduction to Modeling and Optimization*. Springer, 2013.

[7] U. Kiencke and L. Nielsen. *Automotive Control Systems: For Engine, Driveline, and Vehicle*. Springer, 2005.

[8] D. Kum, H. Peng, and N. K. Bucknor. Optimal catalyst temperature management of plug-in hybrid electric vehicles. *American Control Conference*, pages 2732–2738, 2011.

[9] D. Maamria, F. Chaplais, N. Petit, and A. Sciarretta. Numerical optimal control as a method to evaluate the benefit of thermal management in hybrid electric vehicles. In *Proc. of the IFAC World Congress*, pages 4807–4812, 2014.

[10] D. Maamria, F. Chaplais, N. Petit, and A. Sciarretta. On the impact of model simplification in input constrained optimal control: application to HEV energy-thermal management. *53rd IEEE Conference on Decision and Control*, pages 2529–2535, 2014.

[11] F. Merz, A. Sciarretta, J. C. Dabadie, and L. Serrao. On the optimal thermal management of hybrid-electric vehicles with heat recovery systems. *Oil and Gas Science and Technology*, 67(4):601 – 612, 2012.

[12] P. Michel, A. Charlet, G. Colin, Y. Chamaillard, C. Nouillant, and G. Bloch. Energy management of HEV to optimize fuel consumption and pollutant emissions. *Proc of International Symposium on Advanced Vehicle Control*, 2012.

[13] P. Michel, A. Charlet, G. Colin, Y. Chamaillard, C. Nouillant, and G. Bloch. 3 WCC temperature integration in a gasoline-HEV optimal energy management strategy. *Advances in Mechanical Engineering*, 2014.

[14] P. Michel, A. Charlet, G. Colin, Y. Chamaillard, C. Nouillant, and G. Bloch. Catalytic converter modeling for optimal gasoline-HEV energy management. *Proc. of the IFAC World Congress*, pages 6636–6641, 2014.

[15] T. M. Padovani, M. Debert, G. Colin, and Y. Chamaillard. Optimal energy management strategy including battery health through thermal management for hybrid vehicles. *Advances in Automotive Control*, 2013.

[16] L. S. Pontryagin, V. G. Boltyanskii, R. V. Gamkrelidze, and E. F.

Mishchenko. *The mathematical theory of optimal processes*. Interscience Publishers John Wiley & Sons, Inc. New York, London, 1962.

[17] S. Roberts and J. Shipman. Two-point boundary value problems : shooting methods. *American Elsevier Pub, Co, New York*, 1972.

[18] G. Rousseau, D. Sinoquet, A. Sciarretta, and Y. Milhau. Design optimisation and optimal control for hybrid vehicles. *Proc of International Conference on Engineering Optimization*, 2008.

[19] A. Sciarretta, D. di Domenico, P. Pognant-Gros, and G. Zito. *Optimal Energy Management Of Automotive Battery Systems Including Thermal Dynamics and Ageing*. Springer International Publishing, 2014.

[20] L. Serrao, S. Onori, A. Sciarretta, Y. Guezennec, and G. Rizzoni. Optimal energy management of hybrid electric vehicles including battery aging. *Amercan Control Conference*, pages 2125 – 2130, 2011.

[21] L. Serrao, A. Sciarretta, O. Grondin, A. Chasse, Y. Creff, D. di Domenico, P. Pognant-Gros, C. Querel, and L. Thibault. Open issues in supervisory control of hybrid electric vehicles: A unified approach using optimal control methods. In *Int. Scient. Conf. on hybrid and electric vehicles RHEVE 2011*. IFPEN, 2011.

[22] K. van Berkel, W. Klemm, T. Hofman, B. Vroemen, and M. Steinbuch. Optimal energy management for a mechanical-hybrid vehicle with cold start conditions. *European Control Conference*, pages 452–457, 2013.

[23] K. van Berkel, W. Klemm, T. Hofman, B. Vroemen, and M. Steinbuch. Optimal control of a mechanical hybrid powertrain with cold start conditions. *IEEE Transactions on Vehicular Technology*, 63:1555 – 1566, May 2014.